

# SuperMix: Supervising the Mixing Data Augmentation

Ali Dabouei, Sobhan Soleymani, Fariborz Taherkhani, Nasser M. Nasrabadi

West Virginia University

{ad0046, ssoleyma, ft0009}@mix.wvu.edu, nasser.nasrabadi@mail.wvu.edu

**Abstract.** In this paper, we propose a supervised mixing augmentation method, termed SuperMix, which exploits the knowledge of a teacher to mix images based on their salient regions. SuperMix optimizes a mixing objective that considers: i) forcing the class of input images to appear in the mixed image, ii) preserving the local structure of images, and iii) reducing the risk of suppressing important features. To make the mixing suitable for large-scale applications, we develop an optimization technique, 65× faster than gradient descent on the same problem. We validate the effectiveness of SuperMix through extensive evaluations and ablation studies on two tasks of object classification and knowledge distillation. On the classification task, SuperMix provides the same performance as the advanced augmentation methods, such as AutoAugment. On the distillation task, SuperMix sets a new state-of-the-art with a significantly simplified distillation method. Particularly, in six out of eight teacher-student setups from the same architectures, the students trained on the mixed data surpass their teachers with a notable margin<sup>1</sup>.

## 1 Introduction

A principal approach for improving the generalization of deep neural networks (DNNs) is data augmentation which enlarges the training set by transforming images in the given dataset. The classical data augmentation performs a fixed combination of random transformations, such as horizontal flip, crop, scale, color manipulation, and cut out, on the input images [1,2,3]. Recently, notable efforts have been devoted to improving the augmentation, *e.g.*, by automating the search for the optimal augmentation policies [4,5,6,7]. Most of the previous augmentation methods have focused on transforming single images while ignoring the potentially very useful combination of multiple images for the augmentation.

To address this shortcoming, several recent studies have considered merging multiple images for the augmentation [8,9,10,11,12,13]. The performance of these methods is restricted by the lack of supervision, preventing them from exploiting the full potential of input images. Consequently, the current mixing functions are not rigorous enough and often suppress visual patterns by averaging or covering features in one image with the trivial features, *e.g.*, from the background,

---

<sup>1</sup> The code is available at <https://github.com/alldbi/SuperMix>

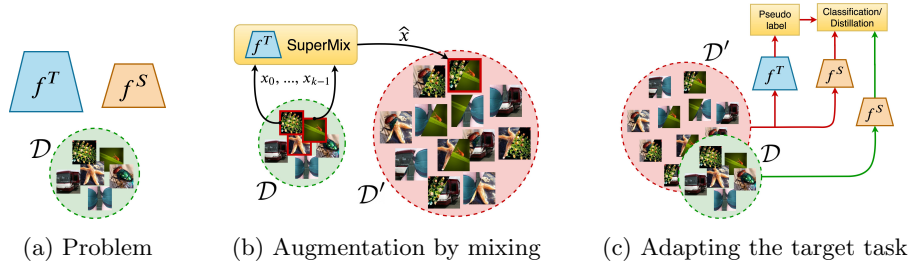


Fig. 1: Overview of how SuperMix can assist the classification or distillation. In the classification task, the teacher is the student model pretrained on  $\mathcal{D}$ .

in another image. The lack of supervision further constrains the performance of training on the mixed images since the corresponding pseudo labels are not accurate. Mixing images from the same class can alleviate this issue but significantly reduces the diversity of the produced images. The knowledge of a teacher can be employed to address these issues by devising a more comprehensive mixing function and producing accurate soft labels for the mixed images.

In this paper, we propose a supervised mixing augmentation method, termed SuperMix, which exploits the knowledge of a teacher to mix input images based on their salient regions. Here, the teacher can be the target model itself pretrained on the original dataset, *i.e.*, self-training [14,15,16,17,18,19], or a more sophisticated model aiming to guide a student network via knowledge transfer [20,21]. We formalize the problem of supervised mixing augmentation by employing a set of mixing masks associating the pixel value at each spatial location in the mixed image to the pixel values at the corresponding location in the input images. Using the masks, we define a general mixing function which, in contrast to previous methods, allows multiple input images to be combined locally. The proposed optimization problem for finding the mixing masks considers three conditions to produce invaluable mixed images. First, the Top- $k$  predicted classes by the teacher for the mixed image must contain the predicted class for each of  $k$  input images. This assures that important features of all images are preserved in the mixing process. Second, the masks must be spatially smooth so that the mixed images resemble the structure of the input images. Third, elements of the masks at each spatial location must be sparse across the input samples to reduce the risk of suppressing important features. This enforces each spatial location in the mixed image to be assigned to a single input image.

Due to the complexity of the problem, optimizing the masks using Stochastic Gradient Descent (SGD) is severely time-consuming and infeasible, especially for large-scale datasets. Therefore, we develop an iterative algorithm for SuperMix that provides  $65\times$  speed-up as compared to SGD, on ImageNet. Through extensive experiments and ablation studies on two tasks of object classification and knowledge distillation, we validate the effectiveness of SuperMix and demonstrate that it exposes knowledge of the teacher by producing rich mixed images with intrinsically smooth soft labels. SuperMix illustrates similar performance to the SOTA automated augmentation methods [4,5,6]. Furthermore, training

the students to merely classify the SuperMix data surpasses the previous complex SOTA methods of distillation with a notable margin. Figure 1 provides an overview of how SuperMix can be incorporated into the training phase of DNNs.

## 2 Related work

**Data augmentation.** Cubuk *et al.* proposed AutoAugment (AA) [4] to automate the search for augmentation policies given a predefined set of transformations and the dataset. Although AA has demonstrated significant performance, it requires prohibitive training time even for small datasets. Hence, multiple approaches have attempted to reduce the training time of the automated augmentation by employing more efficient search approaches, *e.g.*, density matching in fast AutoAugment (FAA) [5], or population-based augmentation (PBA) [6].

Several recent studies have considered employing multiple images for the data augmentation [8,10,11,12,13]. Smart Augmentation [8] proposed merging multiple images from the same class using a DNN trained concurrently with the target model. However, training an additional deep model alongside every target model is resource exhaustive and severely limits the scalability of the approach for large-scale problems. Moreover, the method is restricted to merge images from the same class which limits the diversity and novelty of visual patterns in the merged images. MixUp [10,13] combined a pair of images for the augmentation by convex linear interpolation. CutMix [12] proposed overlaying a cropped area of an input image on another image to augment the data. Although MixUp and CutMix have demonstrated notable improvements to the training of object recognition models, they suffer from major shortcomings discussed in the previous section.

**Knowledge distillation.** In this study, we demonstrate that SuperMix is specifically beneficial for the task of knowledge distillation. Therefore, in this section, we briefly review its background. Bucilua *et al.* [20] proposed utilizing knowledge of the teacher by matching the logits, *i.e.*, outputs before the softmax normalization, of the teacher and the student. Hinton *et al.* [21] pointed out that the decision of the teacher regarding classes other than the winner contains significant information. To better harness this information, they introduced a temperature coefficient in softmax to smooth out the probability predictions before the matching. Since then, many approaches have been proposed for KD [21,22,23,24,25,26,27,28,29,30,31,32,33].

Attention transfer (AT) [24] and FitNet [23] proposed employing the intermediate representations of the teacher, in addition to the outputs, to guide the student. Ahn *et al.* [27] proposed variational information distillation (VID) which maximizes a lower bound to the mutual information between the teacher and the student. Recently, Tian *et al.* [22] proposed contrastive representation distillation (CRD) which maximizes a tighter lower-bound to the mutual information via a contrastive loss. They have benchmarked dozen of the SOTA methods on knowledge distillation and illustrated that CRD outperforms all previous methods of distillation. Although authors have employed a memory buffer to improve the practical feasibility of the theory, CRD requires embedding representations

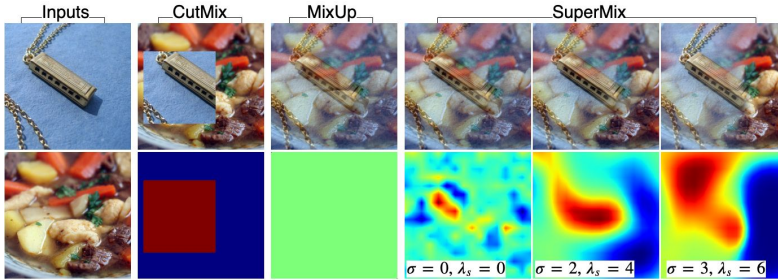


Fig. 2: Visual demonstration of the role of masks in the mixing. First column from the left shows the input images, and the rest of columns show the mixed images and the mixing masks corresponding to the ‘harmonica’.

for a large number of training samples in each iteration. However, we demonstrate that augmenting the training set allows us to achieve SOTA performance with a simple distillation methodology.

### 3 Mixing data augmentation

Mixing augmentation [10,11,12,13] has a great potential for increasing the size of the training sets. Formally, given a training set  $\mathcal{D} = \{(x_i, y_i)\}_{i=0}^{N-1}$ , mixing methods take a subset  $X \subset \mathcal{D}$  to produce a mixed data point  $\hat{x}$  and the label  $\hat{y}$ . A crucial property of mixed images is that they must reside close to the manifold of the training data since the goal of the mixing is to enlarge the support of the training distribution. Previous mixing methods [10,13] have considered this requirement by employing operations that preserve local smoothness of images. MixUp [10,13] combines a pair of images  $(x_i, x_j)$  using convex linear interpolation as:  $\hat{x} = rx_i + (1-r)x_j$ , where  $r \sim \text{Beta}(\alpha, \alpha)$  is a random mixing weight from the symmetric Beta distribution with  $\alpha \in (0, \infty)$ . Due to the lack of supervision, the soft label for  $\hat{x}$  is also computed using the same linear interpolation as:  $\hat{y} = r\delta(y_i) + (1-r)\delta(y_j)$ , where  $\delta(\cdot)$  is the one-hot encoding function. Although this approach and its variants [12,11] have demonstrated effectiveness for training deep models, they suffer from two shortcomings consequences of the blind mixing. First, coefficient  $r$  assigns equal importance to the whole image which can suppress important features by averaging with the background or less important features from the other image. Second, the computed soft label does not accurately describe the probability of classes represented by the mixed image and, thus, negatively affects the training performance.

To address these issues, we formalize a general formulation for the augmentation function. To this aim, we use a set of mixing masks  $M = \{m_i\}_{i=0}^{k-1}$ , where  $m_i : \Lambda \rightarrow [0, 1]$  associates each spatial location  $u \in \Lambda$  in  $x_i$  with a scalar value  $m_i(u)$ . Using the mixing masks, we define the generalized mixing function as:

$$\hat{x} := \sum_{i=0}^{k-1} x_i \odot m_i, \quad (1)$$

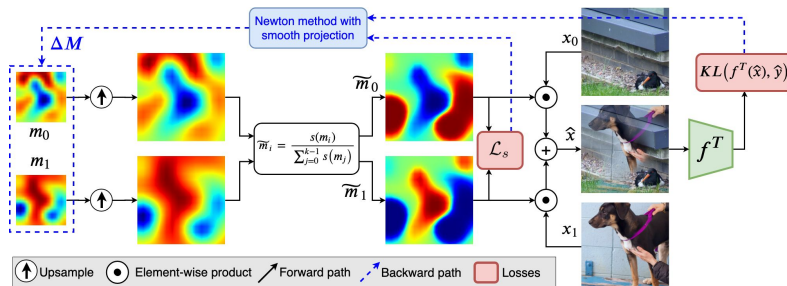


Fig. 3: Schematic diagram of the proposed method for mixing input samples ( $k = 2$ ) using the supervision of the teacher.

where  $x_i$  is the  $i^{\text{th}}$  sample in  $X$ , the operator  $\odot$  denotes the element-wise product, and  $\sum_i m_i(u) = 1$  to hold the convexity of the combination. The mixing function recovers MixUp [10] when  $k = 2$  and all values in each mask are equal. It also recovers CutMix [12] when  $k = 2$  and all values except the cropped area in one of the masks are equal to one. Figure 2 provides a visual comparison of the role of the masks in the mixing augmentation. In the next section, we describe how the knowledge of a teacher model can be used to compute  $M$  such that the mixed image,  $\hat{x}$ , encompasses the rich visual information of samples in  $X$ .

### 3.1 Supervised mixing

In the image classification task, information of categories is embedded in spatial patterns that describe the visual characteristics of each class. The performance of a DNN highly depends on how well it can exploit these spatial features to recognize categories. Therefore, we postulate that incorporating knowledge of a trained model (teacher) to identify and combine salient regions of multiple images can guide the target model (student) to learn more discriminative and generalizable features. Moreover, employing the supervision allows us to address the shortcomings of the blind mixing discussed in the previous section.

Here, we develop a supervised method for mixing input images. Let  $f^T = [f_0^T, \dots, f_{m-1}^T]^T : \mathbb{R}^{W \times H \times C} \rightarrow [0, 1]^m$  denote the probability vector predicted by the teacher for  $m$  classes. Our goal is to optimize the set of masks  $M$  in Equation 1 such that all salient regions in  $X$ , according to the knowledge of the teacher, be present in the mixed image,  $\hat{x}$ . This can be interpreted as:  $f^T(\hat{x}) \approx \hat{y}$ , where  $\hat{y}$  is high for classes associated with images in  $X$ . Hence, we first formulate the target soft label,  $\hat{y}$ , computed in previous approaches [10,12] for  $k = 2$  using the Beta distribution. We generalize this for  $k \geq 2$  by sampling the mixing coefficients from the Dirichlet distribution. Let  $(r_0, \dots, r_{k-1}) \sim \text{Dir}(\alpha)$  be a random sample from the symmetric multivariate Dirichlet distribution with parameter  $\alpha$  and size  $k$ , we define the target soft label as:

$$\hat{y} := \sum_{i=0}^{k-1} r_i \delta(y^T(x_i)), \quad (2)$$

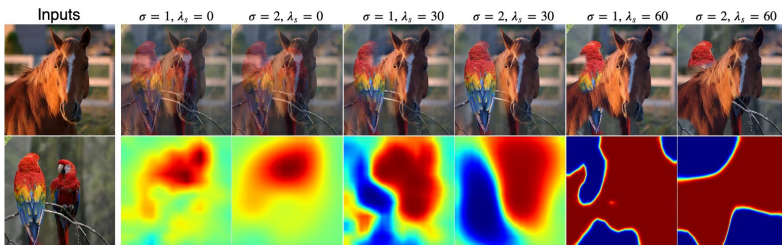


Fig. 4: Visualizing the effect of smoothing factor,  $\sigma$ , and the sparsity promoting weight,  $\lambda_s$ , on the mixed images. Masks are estimated using the supervision of ResNet34 and are associated with the ‘horse’ image.

where  $y^T(x_i) = \arg \max_j f_j^T(x_i)$  is the predicted class by the teacher for  $x_i \in X$ .

Afterward, a set of mixing masks can be found by minimizing  $KL(f^T(\hat{x})||\hat{y})$ , where  $KL$  is the Kullback-Leibler divergence. However, the masks must hold two additional properties to construct rich mixed images. First, generated images must reside close to the manifold of the training data. In practice, this interprets that each mask must be spatially smooth so that the generated images resemble the spatial structure of the inputs. Second, masks must be sparse across the input samples so that each spatial location in the output image is assigned merely to a single image in the input set. This prevents averaging multiple images at each spatial location which can suppress important features. Considering these, the optimization problem for finding the mixing masks can be written as:

$$\arg \min_{m_0, \dots, m_{k-1}} KL(f^T(\hat{x})||\hat{y}) + \lambda_\sigma \mathcal{L}_\sigma(M) + \lambda_s \mathcal{L}_s(M) \quad \text{subject to:} \quad (3)$$

$$1. 0 \leq m_i(u) \leq 1, \quad 2. \sum_i m_i(u) = 1,$$

where  $\mathcal{L}_\sigma$  is a penalty term for the roughness of masks, *e.g.*, total-variation (TV) norm, and  $\mathcal{L}_s$  is a loss function to encourage sparsity of masks across input samples.

Due to the complexity of the task, we develop an iterative algorithm to solve the problem. At each iteration  $t$ , the convexity conditions can be satisfied by the following normalization:

$$\tilde{m}_i^t = \frac{s(m_i^t)}{\sum_{j=0}^{k-1} s(m_j^t)}, \quad (4)$$

where  $s(\cdot)$  is the sigmoid function. Hence, the generalized mixing function in Equation 1 takes the normalized masks to construct  $\hat{x}$ . Using the normalized masks, we define the sparsity promoting loss as:

$$\mathcal{L}_s := \frac{1}{kWH} \sum_{u,i} |\tilde{m}_i^t(u)(\tilde{m}_i^t(u) - 1)|. \quad (5)$$

A proper set of mixing masks can be estimated by minimizing the objective of SuperMix as  $\mathcal{L}_{SM} = KL + \lambda_\sigma \mathcal{L}_\sigma + \lambda_s \mathcal{L}_s$ . A simpler form of this problem has been

**Algorithm 1** SuperMix

---

```

1: inputs: Classifier  $f^T$ , set of  $k$  images  $X$ ,
   low-pass filter  $g_\sigma$ .
2: output: Mixed sample  $\hat{x}$ .
3:  $Y = \{\operatorname{argmax}_j f_j(x_i) : x_i \in X\}$ .
4: Sample  $(r_0, \dots, r_{k-1})$  from  $\operatorname{Dir}(\alpha)$ .
5:  $\hat{y} = \sum_{i=0}^{k-1} r_i \delta(y^T(x_i))$ .
6: Initialize  $(m_0, \dots, m_{k-1}) \leftarrow 0$ ,
    $\hat{x}^0 \leftarrow \frac{1}{k} \sum_{x_i \in X} x_i$ ,  $t \leftarrow 0$ .
7: condition = Top- $k$  predicted classes by  $f(\hat{x}^t)$ 
   are not in  $Y$ .
8: while condition do
9:    $\mathcal{L}'_{SM} = KL(f^T(\hat{x}^t) || \hat{y}) + \lambda_s \mathcal{L}_s$ .
10:   $\widetilde{\Delta}M^t = \frac{-\mathcal{L}'_{SM}}{(g_\sigma * \nabla \mathcal{L}'_{SM})^T \nabla \mathcal{L}'_{SM}} g_\sigma * \nabla \mathcal{L}'_{SM}$ .
11:   $m_i^{t+1} \leftarrow m_i^t + \widetilde{\Delta}m_i$  for  $i \in \{0, \dots, k-1\}$ .
12:   $\widetilde{m}_i^{t+1} = s(m_i^{t+1}) / \sum_{j=0}^{k-1} s(m_j^{t+1})$ .
13:   $\hat{x}^{t+1} \leftarrow \sum_{i=0}^{k-1} x_i \odot \widetilde{m}_i^{t+1}$ .
14:   $t \leftarrow t + 1$ 
15: end while
16: return  $\hat{x}^t$ .

```

---

studied by employing SGD [34] or deep generators [35] for the task of saliency detection and explanation of DNNs predictions. However, the current problem is more complex since multiple images are involved in the optimization and the roughness penalty and sparsity promoting loss should be minimized on all the corresponding masks. As we discussed and evaluated in Section 4.4, SGD is very slow and not feasible for generating a huge amount of data, *e.g.*, multiple times of the size of the original dataset. Furthermore, employing a dedicated deep model to mix data by extending [35] makes the algorithm model-dependent and is not computationally efficient.

We develop a fast and efficient algorithm to optimize the mixing masks based on Newtons iterative method for finding the roots of a nonlinear system of equations in the underdetermined case [36,37]. Specifically, instead of optimizing  $\mathcal{L}_{SM}$ , we optimize  $\mathcal{L}'_{SM} = KL + \lambda_s \mathcal{L}_s$  using a smooth projection (SP) [38] that directly satisfies the smoothness of masks. As we analyze later in Section 4.4, this significantly improves the execution time of the mixing. Considering the first-order approximation of  $\mathcal{L}'_{SM}$  at  $M$ , each mask can be updated at iteration  $t$  to find the roots as:  $m_i^{t+1} \leftarrow m_i^t + \Delta m_i^t$ . The update can be computed using the Newton's method as:

$$\Delta M^t = \frac{-|\mathcal{L}'_{SM}|}{\|\nabla \mathcal{L}'_{SM}\|_2} \nabla \mathcal{L}'_{SM}, \quad (6)$$

where the gradient is with respect to  $M^t$ , the concatenation of  $\{m_0^t, \dots, m_{k-1}^t\}$ . We also have  $|\mathcal{L}'_{SM}| = \mathcal{L}'_{SM}$  since both the divergence and  $\mathcal{L}_s$  are nonnegative. This formulation uses the  $\ell_2$ -norm projection to compute  $\Delta M^t$ . We modify it using SP to preserve the smoothness of masks and compute the smooth update as:

$$\widetilde{\Delta}M^t = \frac{-\mathcal{L}'_{SM}}{(g_\sigma * \nabla \mathcal{L}'_{SM})^T \nabla \mathcal{L}'_{SM}} (g_\sigma * \nabla \mathcal{L}'_{SM}), \quad (7)$$

where  $g_\sigma * \nabla \mathcal{L}'_{SM}$  is a smoothed version of the gradients using the 2D Gaussian smoothing filter  $g$  with the standard deviation  $\sigma$ . It must be noted that all matrices in Equations 6 and 7 are vectorized before the matrix operations, and masks are reshaped back at the end of the iteration. Besides, due to the smoothness of masks, we optimize a down-sampled set of masks and up-sample

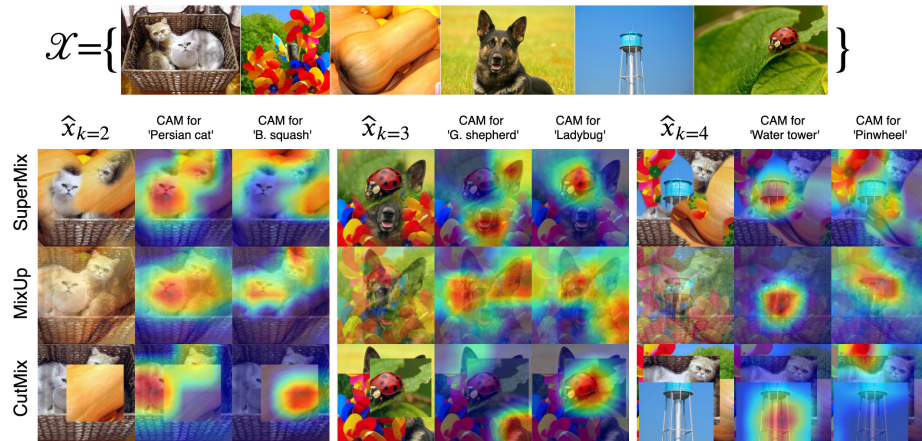


Fig. 5: Visual comparison of the mixed images generated by SuperMix, MixUp, and CutMix, with  $k \in \{2, 3, 4\}$  on ResNet34.

them before performing the mixing. Figure 3 demonstrates a schematic diagram of the proposed mixing approach.

The algorithm terminates when the Top- $k$  predicted classes of  $f^T(\hat{x})$  are the same as the predicted class for samples in  $X$ . For instance, when  $X$  consists of two samples recognized as ‘cat’ and ‘dog’, the Top-2 classes in  $f^T(\hat{x})$  should be classes of ‘cat’ and ‘dog’. This criterion assures that all samples in the input set are visible in the mixed sample according to the knowledge of the teacher. Algorithm 1 and Figure 3 demonstrate the detailed algorithm and schematic diagram for SuperMix, respectively. We perform the algorithm on random sets of input samples drawn from  $\mathcal{D}$  to generate  $\mathcal{D}'$ . For the sake of brevity, we define the augmentation factor  $\kappa = \frac{|\mathcal{D}'|}{|\mathcal{D}|}$  to show the ratio of the size of the mixed dataset over the size of the original dataset. Figure 5 provides a visual comparison of the mixed images produced by SuperMix, MixUp, and CutMix. For a better evaluation, class activation maps [39] are computed for two classes in mixed images.

### 3.2 Training objective

Let  $F^T$  and  $F^S$  denote the logits output of the teacher and the student, respectively. Hinton *et al.* [21] introduced a temperature coefficient,  $\tau$ , for computing the probability outputs as:  $f^T(x, \tau) = \text{softmax}(F^T(x)/\tau)$ , and  $f^S(x, \tau) = \text{softmax}(F^S(x)/\tau)$ . Then, the original objective for the distillation was defined as:

$$\mathcal{L}_{KD}(x) = (1 - \lambda_{KD})\mathcal{H}(f^S(x, 1), y) + \lambda_{KD}\tau^2\mathcal{H}(f^T(x, \tau), f^S(x, \tau)), \quad (8)$$

where  $\mathcal{H}(\cdot, \cdot)$  is the cross-entropy loss function,  $\lambda_{KD}$  is a balancing coefficient, and  $y$  is the ground-truth label of  $x$ . In this setup, all training samples  $x$  are assumed to come from the original dataset  $\mathcal{D}$ . We observed that training the student concurrently on  $\mathcal{D}$  and  $\mathcal{D}'$  using the cross-entropy loss function with equal



Dataset	Model	Base.	Cut.[3]	Automated aug.			Mixing aug.		
				AA[4]	PBA[6]	FAA[5]	MixUp	CutMix	SuperMix
CIFAR-100	WRN-40-2 <sub>a</sub>	26.0	25.2	20.7	-	20.6	22.8	22.1	<b>20.3</b>
	WRN-28-10	18.8	18.4	17.1	16.7	17.3	17.9	17.1	<b>16.4</b>
	S-S(26 2×96d)	17.1	16.0	<b>14.3</b>	15.3	14.6	15.2	15.0	14.5
ImageNet	ResNet-50	23.7/6.9	-	<b>22.4/6.2</b>	-	<b>22.4/6.3</b>	23.0/6.6	22.8/6.5	<b>22.4/6.3</b>
	ResNet-200	21.5/5.8	-	20.0/5.0	-	19.4/4.7	20.4/5.2	20.1/5.1	<b>19.2/4.6</b>

Table 1: Comparing the performance of augmentation methods on CIFAR-100 (Top-1 error) and ImageNet (Top-1/Top-5 errors). Average over 4 independent runs.

weights for the datasets is sufficient to achieve SOTA performance. Therefore, we consider the simple cross-entropy loss for the classification and the distillation tasks as:

$$\mathcal{L}_{CE}(x, \hat{x}) = \mathcal{H}(f^S(x, 1), y) + \mathcal{H}(f^S(\hat{x}, 1), y^T(\hat{x})), \quad (9)$$

where  $y^T(\hat{x})$  is the pseudo label generated by the teacher. We also evaluate the performance of the original distillation enhanced by the augmented datasets by minimizing  $\mathcal{L}_{KD}$  on both the training set and the augmented set.

## 4 Experiments

We evaluate the performance of SuperMix on two tasks of object classification and knowledge distillation [20,21] using two benchmark datasets of CIFAR-100 [1] and ImageNet [40]. For knowledge distillation, we compare SuperMix with four major previous SOTA methods and two mixing augmentation techniques. For the sake of fair comparison, we compute the pseudo label for the data of MixUp and CutMix using the knowledge of the teacher. We also follow the standard setup of evaluation for automated augmentation[4,5,6] and compare them with SuperMix on the task of object classification. For knowledge distillation on CIFAR-100, we also consider an additional baseline by using unlabeled data from the training set of ImageNet32x32 [41] (ImgNet32) to construct unlabeled sets. This helps to better evaluate the role of the data provided by the mixing augmentation methods.

For the distillation, we follow the training setup defined by Tian *et al.* [22]. On CIFAR-100, we use SGD optimizer with learning rate of 0.1 and momentum of 0.9, and weight decay of  $5e-4$ . The learning rate is decayed by 0.1 at epochs 200, 300, 400, and 500, and the maximum number of epochs is set to 600. We also follow the standard Pytorch practice with 10 additional epochs for training on ImageNet. The number of epochs according to the mixed dataset is scaled with  $\frac{1}{\kappa}$ . For instance, when  $\kappa = 5$ , the maximum number of epochs for the mixed dataset is 120. The batch size is set to 128 and 256 for CIFAR-10 and ImageNet, respectively. For the CIFAR-100 dataset, we set  $\sigma$  of the Gaussian smoothing in SuperMix to 1 and the spatial size of the masks to  $8 \times 8$ . For ImageNet,  $\sigma$  is set to 2 and the size of masks is set to  $16 \times 16$ . For all benchmark comparisons, we set  $\tau = 4$ ,  $\alpha = 3$ ,  $\lambda_{KD} = 0.1$ , and  $\lambda_s = 25$ . Moreover, in all experiments, the performance of SuperMix is evaluated by generating  $5 \times 10^5$  and  $10^6$  images on

Teacher	WRN-40-2 <sub>b</sub>		ResNet56	ResNet110		ResNet32x4	VGG13
Student	WRN-16-2	WRN-40-1	ResNet20	ResNet20	ResNet32	ResNet8x4	VGG8
Teacher	75.61		72.34	74.31		79.42	74.64
Student	73.26	71.98	69.06	69.06	71.14	72.50	70.36
KD [21]	74.92	73.54	70.66	70.67	73.08	73.33	72.98
AT [24]	74.08	72.77	70.55	70.22	72.31	73.44	71.43
VID [27]	74.11	73.30	70.38	70.16	72.61	73.09	71.23
CRD [22]	75.48	74.14	71.16	71.46	73.48	75.51	73.94
CRD+KD	75.64*	74.38	71.63	71.56	73.75	75.46	74.29
$\mathcal{L}_{CE}^+$	ImgNet32	74.91	74.80	71.38	71.48	73.17	73.95
	MixUp	76.20*	75.53	72.00	72.27	74.60*	76.73
	CutMix	76.40*	75.85*	72.33	72.68	74.24	76.81
	SuperMix	<b>76.93*</b>	<b>76.11*</b>	<b>72.64*</b>	<b>72.75</b>	<b>74.80*</b>	<b>77.16</b>
$\mathcal{L}_{KD}^+$	ImgNet32	76.52*	75.70*	72.22	72.23	74.24	76.46
	MixUp	76.58*	76.10*	72.89*	72.82	74.94*	77.07
	CutMix	76.81*	76.45*	72.67*	72.83	74.87*	76.90
	SuperMix	<b>77.45*</b>	<b>76.53*</b>	<b>73.19*</b>	<b>72.96</b>	<b>75.21*</b>	<b>77.59</b>

Table 2: Classification performance (%) of student models on CIFAR-100. Teacher and student share the same network architecture. We denote by  $\star$  results where the student surpasses the teacher performance. Only ImgNet32 uses unlabeled data from an external source. Average over 4 independent runs.

CIFAR-100 and ImageNet, respectively, unless otherwise noted. All the hyperparameters are selected according to the experimental setup of [22] and the ablation studies in Section 4.3. Network architectures, settings for the baseline methods, and more training details are provided in the supplemental material.

#### 4.1 Object classification

To provide the supervision for MixUp, CutMix, and SuperMix, we first train the target model on the original dataset and then use it to generate mixed data with  $k$  equal to 2 and 3 for CIFAR-100 and ImageNet, respectively. Afterward, we train the target model from scratch on the mixture of the augmented data and the original data using  $\mathcal{L}_{CE}$  in Equation 9. The rest of the results are reported from the original papers. Table 1 presents the results for these experiments. On four out of five network architectures, SuperMix provides similar results to the SOTA approaches of automated augmentation. This highlights the effectiveness of mixing multiple images for the data augmentation.

#### 4.2 Knowledge Distillation

**Results on CIFAR-100** Tables 2 and 3 presents the results for two challenging scenarios of distillation where teachers and students are and are not from the same architecture, respectively. Training the students to classify the data generated by the mixing augmentation methods consistently outperforms previous methods in both distillation scenarios. The data generated by SuperMix demonstrates the best performance across all evaluations, and, on five out of seven teacher-student setups from the same architecture, students trained on the SuperMix data outperform their teachers. Last five rows in Tables 2 and 3 present the results for knowledge distillation using the original KD [21]. Interestingly, even using the unlabeled data of ImgNet32 with KD outperforms

Teacher	VGG13	ResNet50		ResNet32x4		WRN-40-2 <sub>b</sub>	
Student	MobileNetV2	MobileNetV2	VGG8	ShuffleNetV1	ShuffleNetV2	ShuffleNetV1	
Teacher	74.64	79.34		79.42		75.61	
Student	64.60	64.60	70.36	70.50	71.82	70.50	
KD [21]	67.37	67.35	73.81	74.07	74.45	74.83	
AT [24]	59.40	58.58	71.84	71.73	72.73	73.32	
VID [27]	65.56	67.57	70.30	73.38	73.40	73.61	
CRD [22]	69.73	69.11	74.30	75.11	75.65	76.05*	
CRD+KD	69.94	69.54	74.58	75.12	76.05	76.27*	
$\mathcal{L}_{CE}^+$	ImgNet32	68.85	68.01	73.96	76.80	77.56	75.87*
	MixUp	71.13	71.71	75.41	78.16	78.84	77.29*
	CutMix	70.93	70.64	75.84	77.89	79.32	77.50*
	SuperMix	<b>71.65</b>	<b>72.13</b>	<b>76.07</b>	<b>78.47</b>	<b>79.53*</b>	<b>77.92*</b>
$\mathcal{L}_{KD}^+$	ImgNet32	69.14	68.44	74.32	76.87	77.90	76.23*
	MixUp	71.29	71.99	75.59	78.22	79.14	77.44*
	CutMix	71.10	70.93	76.01	77.92	79.53*	77.65*
	SuperMix	<b>71.81</b>	<b>72.40</b>	<b>76.28</b>	<b>78.51</b>	<b>79.80*</b>	<b>78.07*</b>

Table 3: Classification performance (%) of student models on CIFAR-100. Teacher and student models are from different architectures. We denote by  $\star$  results where the student surpasses the teacher performance. Average over 4 independent runs.

the combination of CRD+KD when networks share the same architecture. The results on MixUp, CutMix, and SuperMix demonstrate that they can enhance the performance of other distillation techniques.

These observations highlight three crucial points. First, the limited size of the training set is a major factor constraining the performance of knowledge distillation. According to Table 2, almost all of the students achieve comparable results to CRD when external data of ImgNet32 is provided. Second, mixing augmentation provides more informative data for the distillation compared to unlabeled data from an external source. Third, the supervised mixing results in rich images that are highly favorable for the task of knowledge distillation and outperforms blind mixing methods.

**Results on ImageNet** We showcase the effectiveness of the mixed data on ImageNet by distilling the knowledge of ResNet-34 into ResNet-18. Table 4 presents the results for the distillation on the ImageNet dataset. Classifying the data generated by the mixing augmentation methods and labeled by the teacher model consistently outperforms the previous SOTA approach with a significant margin. More importantly, in five out of eight experiments of distillation using mixed images, the student outperforms the teacher. This demonstrates the scalability and effectiveness of the mixing augmentation for the task of knowledge distillation. Moreover, combining distillation with the original distillation objective further enhances the distillation performance and validates the effectiveness of the mixing augmentation for enhancing the performance of other distillation methods.

### 4.3 Ablation studies

**Impact of the size of the training set:** In this part, we investigate how the size of the dataset affects the distillation performance by measuring the Top-1 test accuracy of the students versus the augmentation size on CIFAR-100. For

	Teacher Student		AT	KD	CRD		MixUp <sup>(2)</sup>		CutMix <sup>(2)</sup>		SuperMix <sup>(2)</sup>		SuperMix <sup>(3)</sup>	
					$\mathcal{L}_{CE}$	$\mathcal{L}_{KD}$	$\mathcal{L}_{CE}$	$\mathcal{L}_{KD}$	$\mathcal{L}_{CE}$	$\mathcal{L}_{KD}$	$\mathcal{L}_{CE}$	$\mathcal{L}_{KD}$	$\mathcal{L}_{CE}$	$\mathcal{L}_{KD}$
Top-1	26.69	30.25	29.30	29.34	28.83	28.62	26.97	26.71	26.82	26.67*	26.58*	26.38*	26.35*	<b>26.17*</b>
Top-5	8.58	10.93	10.00	10.12	9.87	9.51	8.73	8.56	8.64	8.56*	8.49*	8.34*	8.33*	<b>8.18*</b>

Table 4: Top-1 and Top-5 classification accuracy of ResNet18 on ImageNet dataset. Results where the student surpasses the teacher performance are marked by  $\star$ . Average over 4 independent runs.

all the mixing methods, we set  $k = 2$  and  $\alpha = 1$ , *i.e.*, sampling mixing coefficients from the uniform distribution  $r \sim \text{Unif}(0,1)$ . Figures 6a and 6b present the results for this evaluation conducted on two teacher-student setups. The distillation performance improves by increasing the augmentation size and plateaus at  $5 \times 10^5$ . All the datasets generated using mixing augmentations outperform the unlabeled dataset of ImageNet32. This highlights the superiority of mixed images for knowledge distillation compared to unlabeled data from an external source. Based on these observations, we set the size of the mixed dataset to  $5 \times 10^5$  for all experiments on CIFAR-100.

**Impact of  $\alpha$ :** As depicted in Equation 2,  $\alpha$  determines the probability distribution for the presence of each input class in the mixed image. We measure the performance of distillation versus several values of  $\alpha$  to identify its optimal value. Figures 6c and 6d present the results for these experiments. For  $\alpha \rightarrow 0$ , the mixing augmentation becomes inactive since only one input category will appear in the augmented images, *i.e.*,  $r_0 = 1$  or  $r_1 = 1$ . In this case, the performance of distillation is the same as the case without the augmentation. For  $\alpha \rightarrow +\infty$ , the contribution of images become equal, *i.e.*,  $r_0 = r_1 = 0.5$ . This is more favorable for the distillation since both input images contribute equally to the mixed image. For  $\alpha = 1$ , contribution of each input in the mixed image is selected from the uniform distribution  $\text{Unif}(0, 1)$ . This works better than  $\alpha \rightarrow +\infty$  since not only features of both input images will be present in the output image, but also the number of features from each image will change randomly across mixed images. According to these evaluations, we set  $\alpha = 3$  for all of the experiments, unless otherwise noted.

**Impact of  $k$ :** We evaluate the role of  $k$  by conducting experiments on CIFAR-100 and ImageNet datasets. Figures 6e, 6f, and 6g present the results for this evaluation. A major shortcoming of MixUp and CutMix is that they mix images without any supervision. This explains the notable deterioration of the distillation performance in all experiments with  $k > 2$  using these augmentation methods. Including more input samples to produce a mixed image increases the chance of incorrect cropping in CutMix, and averaging overlapping features in Mixup. Both of these incidents degrade the quality and effectiveness of features in the mixed image, which can also be observed from the visual comparisons provided in Figure 5. However, SuperMix alleviates this issue by considering the supervision of the teacher. We also observe that the spatial size of the image can limit  $k$ . As depicted by Figures 6e and 6f, the performance of distillation on SuperMix images degrades for  $k > 2$  on CIFAR-100 due to the limitation of the

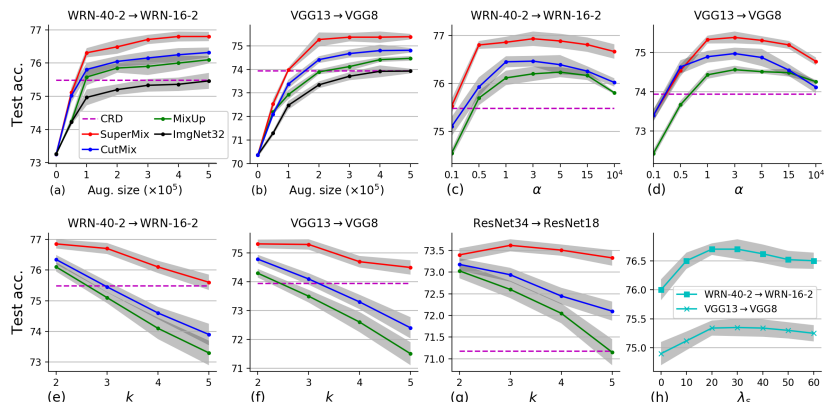


Fig. 6: Evaluating the role of augmentation size and hyper-parameters.

spatial size of  $32 \times 32$ . However on ImageNet, SuperMix with  $k = 3$  yields the best distillation performance.

**Sparsity among masks:** The sparsity promoting loss enforces each spatial location in the output image to be assigned to only one image in the input set. This improves the mixing performance by preserving the most important features in each spatial location. To validate this, we evaluate the performance of distillation versus  $\lambda_s$  in Figure 6h. By increasing the weight of sparsity the performance of distillation improves until  $\lambda_s \approx 25$ . After that the accuracy of masks degrades since the sparsity promoting loss dominates the  $KL$  loss. Figure 4 evaluates this phenomenon by visualising the mixing mask versus  $\lambda_s$ .

#### 4.4 Execution time

We compute the execution time of SuperMix to further evaluate its effectiveness in practice. To this aim, we define two baselines for the sake of comparison. For the first baseline, we use SGD instead of the Newton method to optimize the set of masks. The second baseline is the Newton method without SP. Hence, the optimization in both baselines is performed on  $\mathcal{L}_{SM} = KL + \lambda_\sigma \mathcal{L}_\sigma + \lambda_s \mathcal{L}_s$ . Inspired by the previous work on saliency detection [34], we use the TV norm for the spatial smoothness loss as:  $\mathcal{L}_s = \frac{1}{kWH} \sum_i \sum_{u \in \Lambda} \|\nabla m_i(u)\|_3^3$ . Based on experimental observations, we set  $\lambda_s = 250$ , learning rate of SGD to 0.1. All other parameters are set to the values identified in previous sections. To compute the execution time, all algorithms are implemented with parallel processing on two NVIDIA Titan RTX with a batch size of 128.

Figure 7c presents the results for these comparisons. Newton method with SP, *i.e.*, SuperMix, is at least  $65\times$  faster than SGD on both datasets. Moreover, due to SP which directly satisfied the spatial smoothness condition, SuperMix is at least  $19\times$  faster than the pure Newton iterative method without SP.

#### 4.5 Embedding space evaluations

We perform two sets of evaluations on CIFAR-100 to analyze the characteristics of the mixed images. In the first set of experiments, we feed the original data

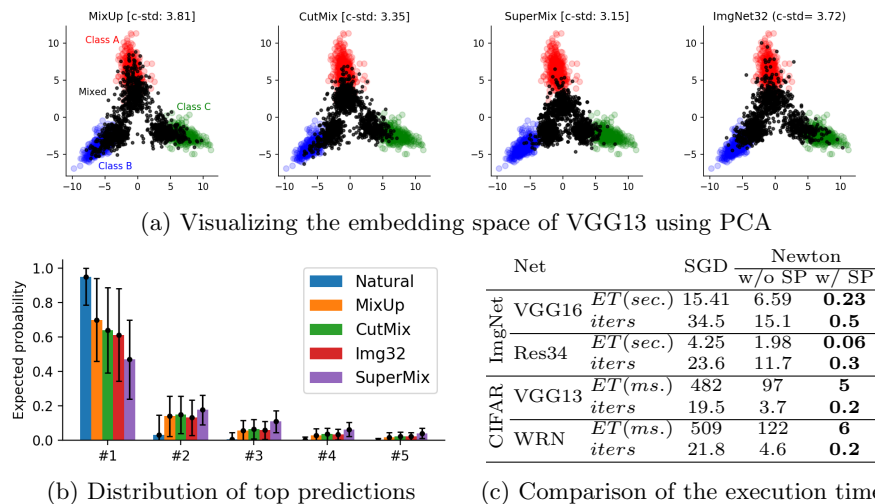


Fig. 7: Evaluating the characteristics of the augmented samples in the embedding space (a, b), and the execution time (c).

and the mixed images to VGG13 and visualize the embedding space, *i.e.*, one layer before the logits layer, for three random classes using PCA in 2D. The SuperMix images are generated with  $k = 2$  using the supervision of VGG13. Figure 7a demonstrates these evaluations. The representations of the SuperMix data has less overlap with the distribution of the representations for the original data. This suggests that the SuperMix data encompass more novel structure compared to the original data, unlabeled data from other mixing methods or an external source. Moreover, the SuperMix data are harder to classify for the model since the representations are concentrated close to the center of the embedding. To better evaluate this, we compute the class standard deviation (c-std) of representations for each class. The computed values are reported on the top of the corresponding images in Figure 7a.

Hinton *et al.* [21] pointed out that smoothed probability predictions of a model can better reveal its knowledge of the task. Since SuperMix generates images by combining multiple inputs, the outputs of the model for the SuperMix data are intrinsically more smooth compared to the outputs for other augmentation types. We validate this by computing the average of the sorted Top-5 probability predictions of VGG13 on the original and augmented images of CIFAR-100. Figure 7b presents the results for this evaluation. As demonstrated in Figure 7b, predictions of the target model is significantly smoother on mixed images. Moreover, SuperMix produces data with the most smooth probabilities.

## 5 Conclusion

In this paper, we have studied the potential of mixing multiple images using the supervision of a teacher for data augmentation. We proposed SuperMix,

a supervised mixing augmentation method that combined multiple images to produce rich data. The effectiveness and efficiency of SuperMix are validated through extensive experiments and evaluations. We demonstrated that SuperMix significantly improves the state-of-the-art of knowledge distillation and provides the same performance as the complex methods of automated augmentation.

## References

1. Krizhevsky, A., Hinton, G., et al.: Learning multiple layers of features from tiny images. Technical report, Citeseer (2009)
2. Han, D., Kim, J., Kim, J.: Deep pyramidal residual networks. In: Proceedings of the IEEE conference on computer vision and pattern recognition. (2017) 5927–5935
3. DeVries, T., Taylor, G.W.: Improved regularization of convolutional neural networks with cutout. arXiv preprint arXiv:1708.04552 (2017)
4. Cubuk, E.D., Zoph, B., Mane, D., Vasudevan, V., Le, Q.V.: Autoaugment: Learning augmentation strategies from data. In: Proceedings of the IEEE conference on computer vision and pattern recognition. (2019) 113–123
5. Lim, S., Kim, I., Kim, T., Kim, C., Kim, S.: Fast autoaugment. In: Advances in Neural Information Processing Systems. (2019) 6662–6672
6. Ho, D., Liang, E., Stoica, I., Abbeel, P., Chen, X.: Population based augmentation: Efficient learning of augmentation policy schedules. arXiv preprint arXiv:1905.05393 (2019)
7. Cubuk, E.D., Zoph, B., Shlens, J., Le, Q.V.: Randaugment: Practical data augmentation with no separate search. arXiv preprint arXiv:1909.13719 (2019)
8. Lemley, J., Bazrafkan, S., Corcoran, P.: Smart augmentation learning an optimal data augmentation strategy. *Ieee Access* **5** (2017) 5858–5869
9. Perez, L., Wang, J.: The effectiveness of data augmentation in image classification using deep learning. arXiv preprint arXiv:1712.04621 (2017)
10. Zhang, H., Cisse, M., Dauphin, Y.N., Lopez-Paz, D.: mixup: Beyond empirical risk minimization. arXiv preprint arXiv:1710.09412 (2017)
11. Guo, H., Mao, Y., Zhang, R.: Mixup as locally linear out-of-manifold regularization. In: Proceedings of the AAAI Conference on Artificial Intelligence. Volume 33. (2019) 3714–3722
12. Yun, S., Han, D., Oh, S.J., Chun, S., Choe, J., Yoo, Y.: Cutmix: Regularization strategy to train strong classifiers with localizable features. arXiv preprint arXiv:1905.04899 (2019)
13. Tokozume, Y., Ushiku, Y., Harada, T.: Between-class learning for image classification. In: Proceedings of the IEEE Conference on Computer Vision and Pattern Recognition. (2018) 5486–5494
14. Scudder, H.: Probability of error of some adaptive pattern-recognition machines. *IEEE Transactions on Information Theory* **11**(3) (1965) 363–371
15. Vapnik, V., Vapnik, V.: *Statistical learning theory* (1998)
16. Rosenberg, C., Hebert, M., Schneiderman, H.: Semi-supervised self-training of object detection models. *WACV/MOTION* **2** (2005)
17. Li, L.J., Fei-Fei, L.: Optimol: automatic online picture collection via incremental model learning. *International journal of computer vision* **88**(2) (2010) 147–168
18. Chen, X., Shrivastava, A., Gupta, A.: Neil: Extracting visual knowledge from web data. In: Proceedings of the IEEE International Conference on Computer Vision. (2013) 1409–1416
19. Yarowsky, D.: Unsupervised word sense disambiguation rivaling supervised methods. In: 33rd annual meeting of the association for computational linguistics. (1995) 189–196
20. Bucilu, C., Caruana, R., Niculescu-Mizil, A.: Model compression. In: Proceedings of the 12th ACM SIGKDD international conference on Knowledge discovery and data mining, ACM (2006) 535–541



21. Hinton, G., Vinyals, O., Dean, J.: Distilling the knowledge in a neural network. arXiv preprint arXiv:1503.02531 (2015)
22. Tian, Y., Krishnan, D., Isola, P.: Contrastive representation distillation. arXiv preprint arXiv:1910.10699 (2019)
23. Romero, A., Ballas, N., Kahou, S.E., Chassang, A., Gatta, C., Bengio, Y.: Fitnets: Hints for thin deep nets. arXiv preprint arXiv:1412.6550 (2014)
24. Zagoruyko, S., Komodakis, N.: Paying more attention to attention: Improving the performance of convolutional neural networks via attention transfer. arXiv preprint arXiv:1612.03928 (2016)
25. Tung, F., Mori, G.: Similarity-preserving knowledge distillation. In: Proceedings of the IEEE International Conference on Computer Vision. (2019) 1365–1374
26. Peng, B., Jin, X., Liu, J., Li, D., Wu, Y., Liu, Y., Zhou, S., Zhang, Z.: Correlation congruence for knowledge distillation. In: Proceedings of the IEEE International Conference on Computer Vision. (2019) 5007–5016
27. Ahn, S., Hu, S.X., Damianou, A., Lawrence, N.D., Dai, Z.: Variational information distillation for knowledge transfer. In: Proceedings of the IEEE Conference on Computer Vision and Pattern Recognition. (2019) 9163–9171
28. Yim, J., Joo, D., Bae, J., Kim, J.: A gift from knowledge distillation: Fast optimization, network minimization and transfer learning. In: Proceedings of the IEEE Conference on Computer Vision and Pattern Recognition. (2017) 4133–4141
29. Park, W., Kim, D., Lu, Y., Cho, M.: Relational knowledge distillation. In: Proceedings of the IEEE Conference on Computer Vision and Pattern Recognition. (2019) 3967–3976
30. Passalis, N., Tefas, A.: Learning deep representations with probabilistic knowledge transfer. In: Proceedings of the European Conference on Computer Vision (ECCV). (2018) 268–284
31. Heo, B., Lee, M., Yun, S., Choi, J.Y.: Knowledge transfer via distillation of activation boundaries formed by hidden neurons. In: Proceedings of the AAAI Conference on Artificial Intelligence. Volume 33. (2019) 3779–3787
32. Kim, J., Park, S., Kwak, N.: Paraphrasing complex network: Network compression via factor transfer. In: Advances in Neural Information Processing Systems. (2018) 2760–2769
33. Huang, Z., Wang, N.: Like what you like: Knowledge distill via neuron selectivity transfer. arXiv preprint arXiv:1707.01219 (2017)
34. Fong, R.C., Vedaldi, A.: Interpretable explanations of black boxes by meaningful perturbation. In: Proceedings of the IEEE International Conference on Computer Vision. (2017) 3429–3437
35. Dabkowski, P., Gal, Y.: Real time image saliency for black box classifiers. In: Advances in Neural Information Processing Systems. (2017) 6967–6976
36. Moosavi-Dezfooli, S.M., Fawzi, A., Frossard, P.: Deepfool: a simple and accurate method to fool deep neural networks. In: Proceedings of the IEEE conference on computer vision and pattern recognition. (2016) 2574–2582
37. Ruszczyński, A.P., Ruszczyński, A.: Nonlinear optimization. Volume 13. Princeton university press (2006)
38. Dabouei, A., Soleymani, S., Taherkhani, F., Dawson, J., Nasrabadi, N.M.: Smoothfool: An efficient framework for computing smooth adversarial perturbations. arXiv preprint arXiv:1910.03624 (2019)
39. Zhou, B., Khosla, A., Lapedriza, A., Oliva, A., Torralba, A.: Learning deep features for discriminative localization. In: Proceedings of the IEEE conference on computer vision and pattern recognition. (2016) 2921–2929

40. Deng, J., Dong, W., Socher, R., Li, L.J., Li, K., Fei-Fei, L.: Imagenet: A large-scale hierarchical image database. In: 2009 IEEE conference on computer vision and pattern recognition, Ieee (2009) 248–255
41. Chrabaszcz, P., Loshchilov, I., Hutter, F.: A downsampled variant of imagenet as an alternative to the cifar datasets. arXiv preprint arXiv:1707.08819 (2017)